



Vein reactivation and complex vein intersection geometries in the Taconic Slate Belt

JEAN M. CRESPI and YU-CHANG CHAN

Department of Geology and Geophysics, 354 Mansfield Road, University of Connecticut, Storrs
CT 06269-2045, U.S.A.

(Received 13 October 1995; accepted in revised form 27 February 1996)

Abstract—This paper describes some complex intersection geometries for veins in the Taconic slate belt of western New England, U.S.A. The complexity is primarily a result of the preferential reactivation during slaty cleavage development of one set of veins within an orthogonal system of pre-cleavage veins. The relative age of the pre-cleavage veins also influences the intersection geometry in that the non-reactivated veins, which form the younger set of pre-cleavage veins, act as barriers to the propagation of the syn-cleavage veins. These types of intersection geometries are easily misinterpreted without microscale observations of vein textures and may be more common than is currently appreciated. Copyright © 1996 Elsevier Science Ltd

INTRODUCTION

Studies of mineral-filled veins have provided information on subjects as widely varying as the earthquake cycle (Davison 1995), metamorphic fluid flow (Ague 1994), ductile flow within shear zones (Wallis 1992) and the relation between deformation and diagenesis in accretionary prisms (Orange *et al.* 1993). The analysis of veins typically includes the determination of cross-cutting relations, either between the veins and various deformation features in the rock or, in the case of multiple sets of veins, between the intersecting veins themselves. Information on the relative age of multiple sets of veins can be particularly helpful in understanding changes through time in fluid-rock interactions and deformation conditions.

Criteria for determining the relative age of intersecting veins are considered so straightforward they have received little attention in the literature, even in review articles on low-grade deformation (Groshong 1988) and small-scale brittle structures (Dunne & Hancock 1994). This view arises, in part, from the assumption that veins undergo relatively simple opening histories, forming as a result of one crack event or a series of crack events related to a single progressive deformation. In this paper, we describe some complex intersection geometries for veins in the Taconic slate belt of western New England, U.S.A. The complexity is a direct result of vein reactivation during slaty cleavage development. The reactivation affects the vein intersection geometry in that the distribution, width and continuity of the syn-cleavage vein fill is strongly influenced by the relative age of the pre-cleavage veins and their geometry with respect to the slaty cleavage strain field. Vein intersection geometries that are affected by reactivation are easily misinterpreted without microscale observations of vein textures; they may, however, be

common, especially in rocks that have undergone several episodes of deformation.

GEOLOGIC SETTING OF THE VEINS

This study is based on meso- and microscale observations of veins exposed in the vicinity of U.S. Highway 4, from about 3 km southwest of the Vermont–New York state border to about 1 km west of Castleton, Vermont. The strata in this area form part of the Taconic sequence, a shale-dominated facies of the Cambro-Ordovician North American passive margin that was imbricated into a series of west-directed thrust sheets during mid Ordovician arc–continent collision (Zen 1961, Chapple 1973, Rowley *et al.* 1979, Stanley & Ratcliffe 1985). The strata are metamorphosed to lower greenschist grade and have been deformed into tight to isoclinal, west-vergent folds. The strata are also characterized by a well developed, moderately east-dipping slaty cleavage that is approximately axial planar to the folds.

HISTORY OF VEIN DEVELOPMENT

The complex vein intersection geometries are the result of a three-stage history of vein development: (1) formation of a N–S striking set of veins that accommodated early bedding-parallel extension, (2) formation of an E–W striking set of veins that also accommodated bedding-parallel extension and (3) preferential reactivation of this orthogonal system of veins during slaty cleavage development.

Early N-S and E-W striking vein sets

The veins, which are composed primarily of calcite, lie both in the slate layers and the interbedded carbonate and sandstone horizons. When viewed on bedding- or cleavage-parallel surfaces, the veins commonly display a seemingly complex array of orientations. When systematically mapped across the area, however, they define two main sets, with a broad range of vein orientations within each set (Fig. 1).

The morphology of the veins in the N-S striking set and their geometric relation to bedding varies with rock type. In the carbonate and sandstone horizons, the veins are relatively thick (5 to 50mm on average), and individual veins may be tapered at one or both ends,

abruptly truncated at compositional interfaces or continuous with veins in the adjacent slate layers. The veins in the carbonate and sandstone horizons also show little evidence of deformation and invariably lie approximately normal to bedding (subset Ia in Fig. 1b). In contrast, the veins in the slate layers are relatively thin (0.5 to 3 mm on average), lie at low to moderate angles to bedding (subset Ib in Fig. 1b) and have generally been extended as shown by well developed boudinage structures.

Veins in the E-W striking set (set II in Fig. 1b) show less variation in morphology and geometric relation to bedding. They more commonly continue across compositional interfaces and are approximately normal to bedding both in the slate layers and carbonate and sandstone horizons. Veins in this set are also deformed as evidenced by the gently folded geometry of many of the veins.

It is quite difficult to determine the relative age of the N-S and E-W striking vein sets. The difficulty results primarily from the extensive modification of the vein intersections during slaty cleavage development and is compounded by the similarity in composition and orthogonal relation of the veins in the two sets. Wherever the relative age can be determined with confidence, however, the veins in the E-W striking set are younger than the veins in the N-S striking set.

A pre-cleavage origin for both sets of veins, which is suggested by the deformation of the veins, is corroborated by the orientation of the veins with respect to the slaty cleavage strain field. The mean orientation of the X, Y and Z axes of the cleavage-related finite strain ellipsoid are shown in Fig. 1(b), assuming slaty cleavage represents the plane of finite flattening, and the well developed mineral elongation lineation represents the maximum finite stretching axis. Neither the N-S striking vein set nor the E-W striking vein set is symmetrically oriented about elements of the slaty cleavage strain field. In particular, the girdle defined by the poles to the veins in the N-S striking set does not lie within the XZ plane, and the mean pole to the veins in the E-W striking set does not parallel the Y -axis. This angular discordance between the veins and elements of the slaty cleavage strain field, although small, implies the veins did not form as cleavage-related extension cracks. Such an interpretation is supported by the geometry of quartz-phyllsilicate fibers in strain fringes around pyrite framboids (Chan & Crespi 1995). In cleavage-parallel sections, the trace of the fibers in the strain fringes is straight and parallel to the mineral elongation lineation, implying no extension in the Y direction and no variation in orientation of the X axis in a cleavage-plane reference frame during the development of the slaty cleavage. Thus, the deformation and orientation of the veins point to a pre- rather than early syn-cleavage origin for the veins.

The following evidence for vein reactivation and examples of vein intersection geometries are from veins developed within the slate layers. All the photographs are oriented so that the veins in the N-S striking set are subvertical, and the veins in the E-W striking set are subhorizontal. The photomicrographs view down onto a cleavage-parallel surface, and the outcrop photograph

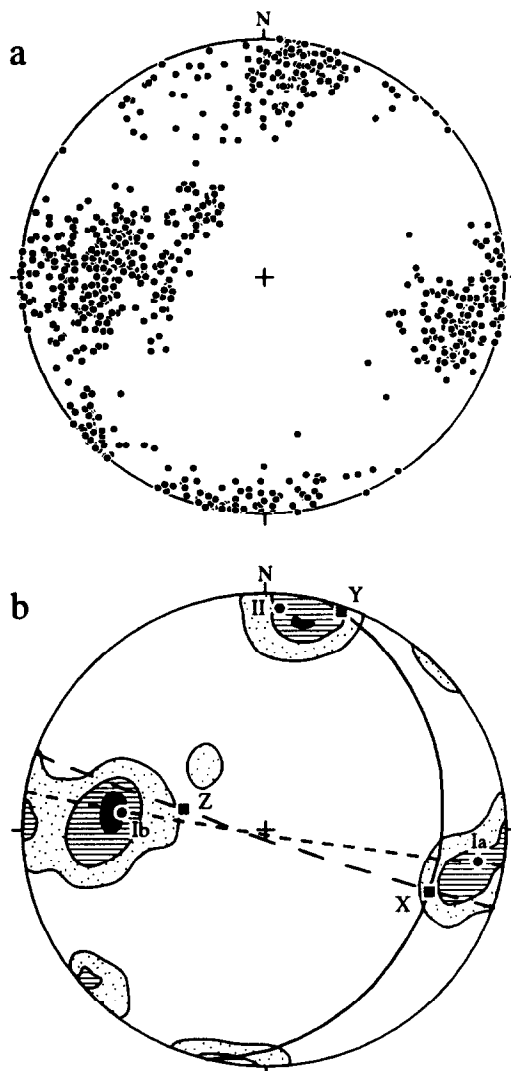


Fig. 1. (a) Poles to veins in study area ($n = 775$). (b) Contour diagram of poles to veins in study area (2%/1% area contour intervals) and relation to X, Y and Z axes of cleavage-related finite strain ellipsoid (XY plane = mean slaty cleavage plane ($n = 517$); X -axis = mean mineral elongation lineation ($n = 34$)). Mean poles to three sets/subsets of veins (Ia, Ib, II) are also shown. Equal-area, lower-hemisphere stereographic projections.

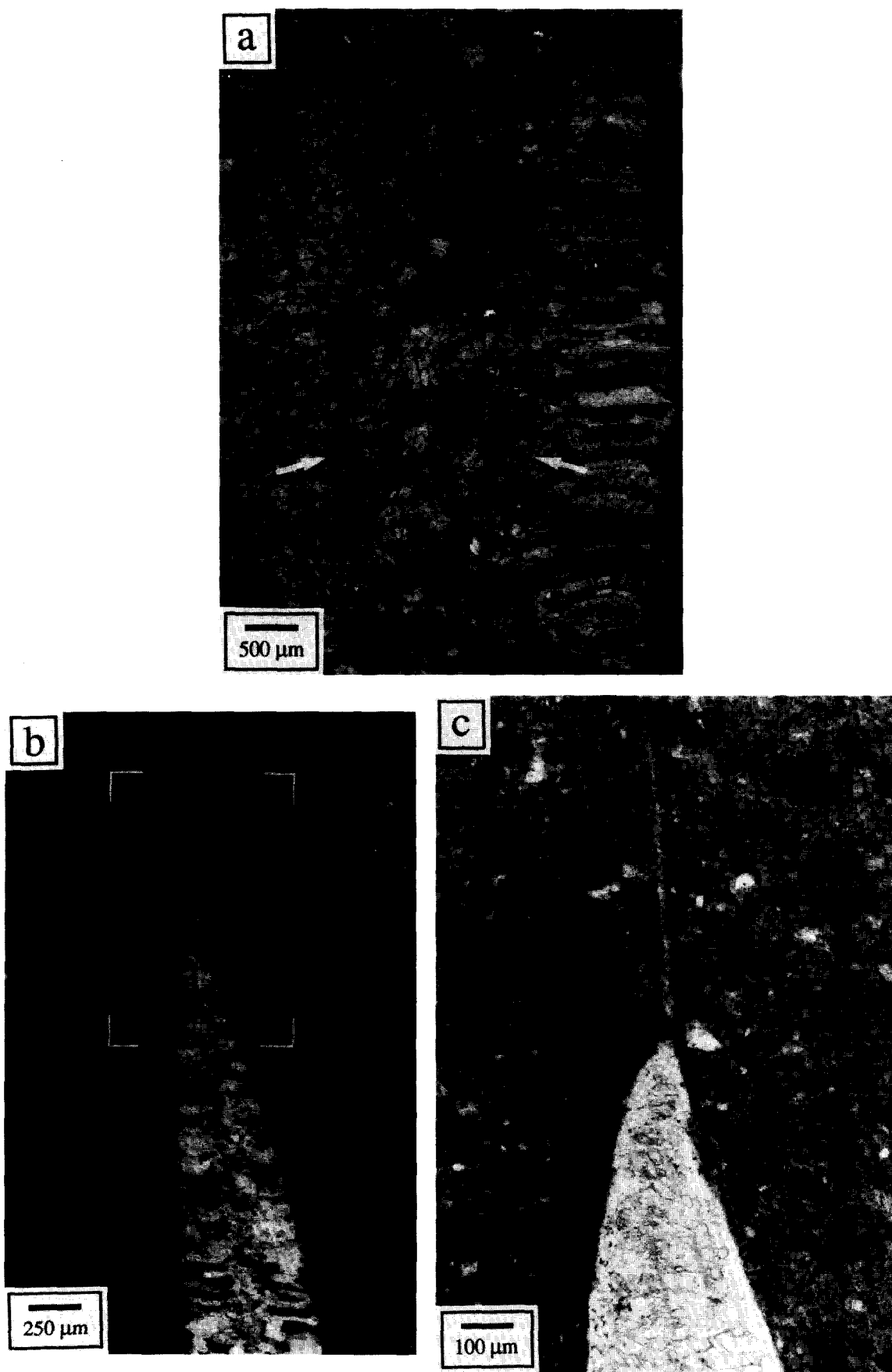


Fig. 2. (a) Photomicrograph of calcite vein consisting of an inner zone of pre-cleavage blocky calcite and an outer zone of syn-cleavage fibrous calcite. Arrows show boundary between pre-cleavage and syn-cleavage vein fill. Crossed polarized light. (b) and (c) Photomicrographs of calcite vein composed of a pre-cleavage microvein and a wide zone of syn-cleavage fibrous calcite. Brackets in (b) show location of (c). Crossed polarized light (b). Plane polarized light (c). Photomicrographs view down onto cleavage-parallel surface. Veins lie in N-S striking set.

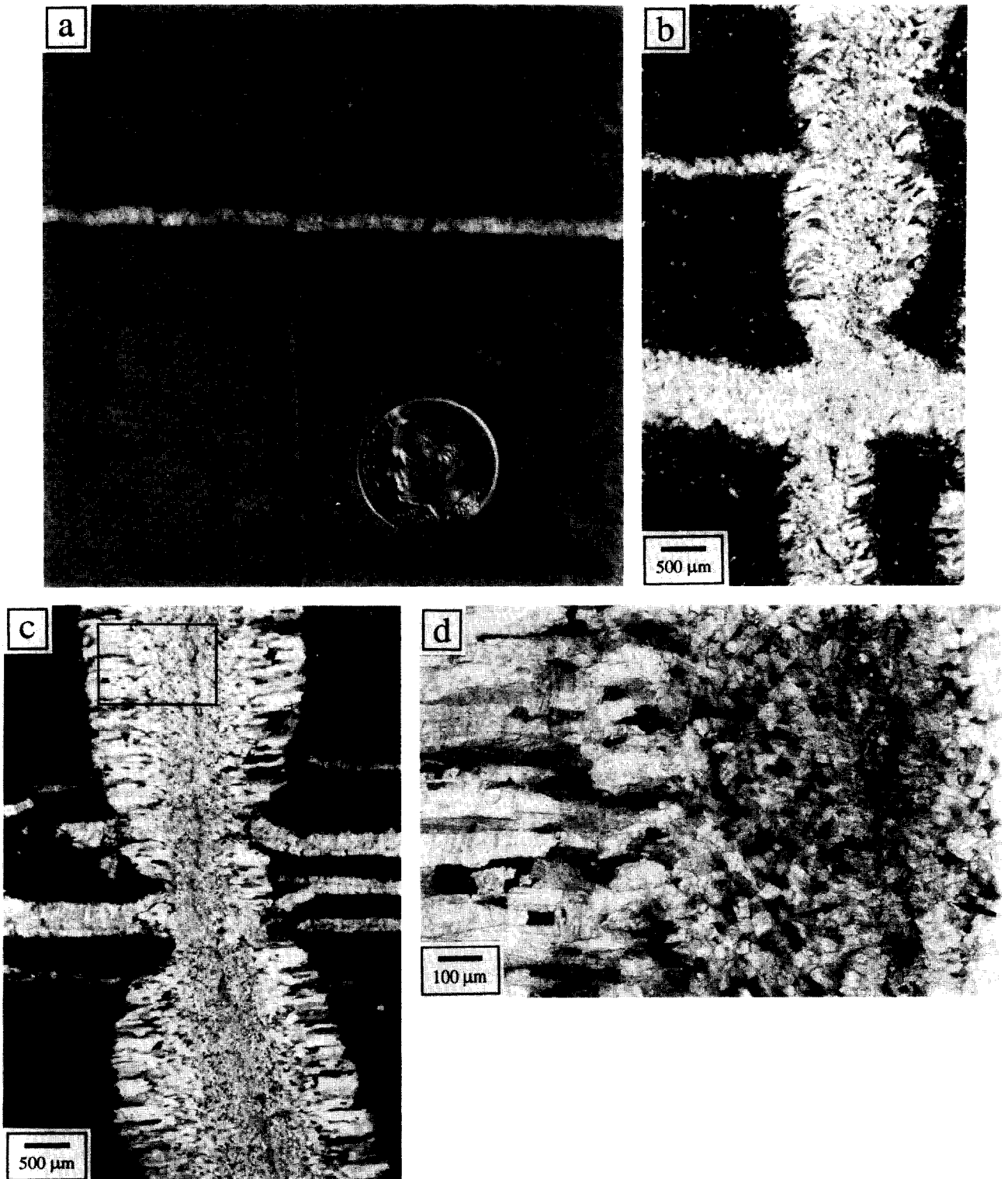


Fig. 3. (a) Outcrop photograph of vein intersection geometry. Diameter of coin = 1.75 cm. (b) and (c) Photomicrographs of vein intersection geometries. Crossed polarized light. (d) Photomicrograph of boxed area shown in (c). Arrows show boundary between pre-cleavage and syn-cleavage vein fill. Crossed polarized light. Outcrop photograph views down onto bedding-parallel surface; photomicrographs view down onto cleavage-parallel surface. Veins in N-S striking set are subvertical; veins in E-W striking set are subhorizontal. See text for discussion.

views down onto a bedding-parallel surface (cleavage and bedding lie at very low angles over most of the area).

Evidence for vein reactivation during slaty cleavage development

The texture of the calcite vein fill provides compelling evidence for reactivation of the veins during slaty cleavage development. In particular, the fill of many of the veins within the slate layers displays two textural zones that lie parallel to the vein walls. The texture of the calcite vein fill in both zones was examined in cleavage-parallel and cleavage-perpendicular sections to avoid sectioning effects. This shows that the texture of the calcite in the inner zone varies from vein to vein (compare, for example, Fig. 2a and Fig. 3d), whereas the texture of the calcite in the outer zone is consistently fibrous. Moreover, in cleavage-parallel sections, the trace of the calcite fibers in the outer zone consistently lies parallel to the mineral elongation lineation in the wall rock, indicating precipitation of the material in the outer zone during slaty cleavage development. In cleavage-perpendicular and lineation-parallel sections, the calcite fibers in the outer zone consistently show clockwise curvature from the inner zone to the vein walls when viewed to the NNE.

Figure 2(a) shows a particularly clear example of this textural zonation. The boundary between the inner and outer zones is quite sharp, with the inner zone consisting of relatively large (100–750 μm) blocky calcite crystals and the outer zone consisting of relatively thin (25 to 150 μm) calcite fibers. (Although some of the material in the outer zone on the left appears blocky, this is simply an artifact of sectioning the curved fibers; the lack of material with a blocky appearance in the outer zone on the right reflects a smaller amount of curvature for the fibers on this side of the vein.)

The vein shown in Fig. 2(b) & (c), in contrast, is not obviously texturally zoned. It appears instead to have all the characteristics of an outer zone, consisting of fibrous calcite with the trace of the fibers parallel to the mineral elongation lineation in the wall rock. The geometry of the tip region of the vein shows, however, that the vein had a two-stage history of development. In particular, the actual end of the vein does not coincide with the abrupt decrease in width of the fibrous calcite vein fill. A very thin (5 to 10 μm) microvein extends for about 1.5 mm beyond the point where the fibrous calcite vein fill terminates. This geometry effectively records the propagation of a syn-cleavage vein along a pre-existing microvein. Vein propagation may have ceased in this particular case because cleavage-related extension was transferred to an en échelon vein (Fig. 4). The textural zonation of the vein is not apparent simply because the pre-existing vein was so narrow.

Overall, the veins in the N–S striking set, which lie at high angles to the X-axis on cleavage-parallel surfaces, were reactivated to a much greater extent than veins in the E–W striking set, which lie at low angles to the X-axis

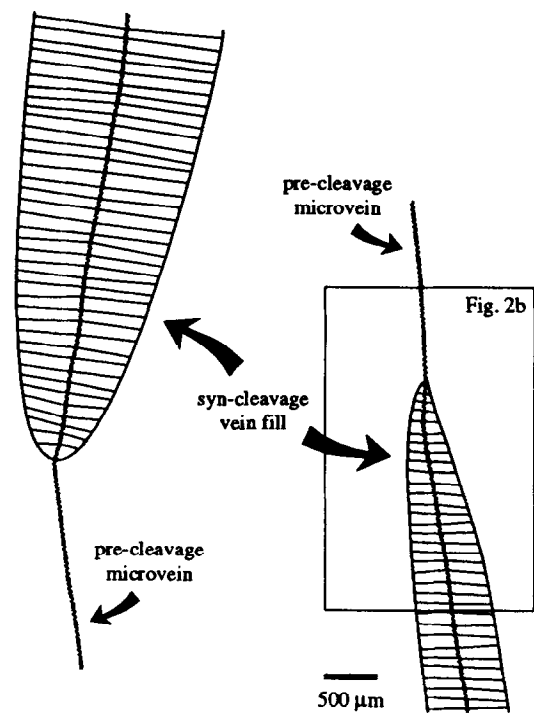


Fig. 4. Sketch of en échelon geometry of two reactivated veins. Both veins are composed of a pre-cleavage microvein and a wide zone of syn-cleavage fibrous calcite. Note abrupt decrease in width of syn-cleavage vein fill in vein overlap area and continuation of microvein beyond point where syn-cleavage vein fill terminates. Box shows location of Fig. 2(b). View is down onto cleavage-parallel surface. Veins lie in N–S striking set.

on cleavage-parallel surfaces. This is shown by the more common existence and greater width of cleavage-related vein fill for veins in the N–S striking set. Veins in the E–W striking set typically have very narrow, and in many cases, no cleavage-related vein fill.

VEIN INTERSECTION GEOMETRIES

Figure 3(a)–(c) show several meso- and microscale examples of vein intersection geometries that have resulted from the three-stage history of vein development outlined above. A common feature of all these examples is the relatively uniform width of the veins in the E–W striking set across the intersection region and the decrease in width of the veins in the N–S striking set directly adjacent to the vein intersection. The variation in width of the veins in the N–S striking set is a direct result of variations in the amount of syn-cleavage fibrous calcite vein fill. This is well shown in Fig. 3(c) where the pre-cleavage vein fill is very narrow (about one-tenth the total vein width; see Fig. 3d for a close-up of the boundary between pre- and syn-cleavage vein material), and the syn-cleavage vein fill abruptly decreases to about half its normal width at the vein intersection region. The veins in the E–W striking set, which show little variation in width, are composed almost entirely of pre-cleavage vein fill.

The examples of vein intersection geometries shown in Fig. 3(a)–(c) differ mainly with respect to the continuity of the veins in the N–S striking set across the vein intersection region. In Fig. 3(a), the N–S striking vein

continues on the opposite side of the E–W striking vein. On either side, however, the N–S striking vein pinches down and appears to terminate a short distance ($< \sim 1$ mm) from the wall of the E–W striking vein, effectively isolating a sliver of wall rock between the veins. In the example in the lower part of Fig. 3(b), the N–S striking vein also continues on the opposite side of the E–W striking vein. In this case, however, the N–S striking vein abuts the E–W striking vein. In contrast, in the example in the upper part of Fig. 3(b), the N–S striking vein actually transects the E–W striking vein. Finally, Fig. 3(c) shows a more complex example in which the N–S striking vein both abuts and transects veins forming the group of closely spaced E–W striking veins.

Both the decrease in width and variation in continuity of the veins in the N–S striking set in the vein intersection region are readily explained in the context of the outlined history of vein development. Of particular significance is the observation that the older set of veins within the orthogonal system of pre-cleavage veins is also the set preferentially oriented for reactivation during slaty cleavage development.

Because the veins in the N–S striking set accommodated syn-cleavage extension by the localized precipitation of new material, whereas the veins in the E–W striking set accommodated syn-cleavage extension by homogeneous deformation, compatibility arguments require a strain gradient across the intersection region. This gradient is expressed by the decrease in width of the syn-cleavage vein fill within the veins in the N–S striking set. The distance over which this gradient occurs varies and probably depends upon the degree of cohesion between the wall rock and E–W striking vein.

In addition, because vein formation during slaty cleavage development involved the progressive opening of the pre-existing veins in the N–S striking set rather than the formation of new cracks, the veins in the E–W striking set essentially acted as barriers to the propagation of the syn-cleavage veins. The extent to which the veins acted as barriers differs, however, and appears to depend upon the width of the vein in the E–W striking set. The vein intersection geometries in Fig. 3(a) and the lower part of Fig. 3(b) show cases in which the vein in the E–W striking set was effective in stopping the propagation of the syn-cleavage vein. The unusual preservation of wall rock between the two veins in Fig. 3(a) is probably a result of two factors: syn-cleavage vein propagation ceasing a short distance from the walls of the E–W striking vein and syn-cleavage vein reactivation occurring along a pre-existing microvein (similar to Fig. 2b & c) that is, in fact, present within the slivers of wall rock between the two veins but is simply not visible at the outcrop scale. The vein intersection geometry in the upper part of Fig. 3(b), in contrast, shows a case in which the E–W striking vein was ineffective in stopping the propagation of the syn-cleavage vein. Unlike the examples in Fig. 3(a) and the lower part of Fig. 3(b), the E–W striking vein in this example is relatively thin. The more complex geometry displayed by the vein intersection region in Fig. 3(c) is a result of the relatively thin but

closely spaced E–W striking veins varying in the extent to which they acted as barriers to the propagation of the syn-cleavage vein.

DISCUSSION

The complex vein intersection geometries described in this paper result primarily from the preferential reactivation during slaty cleavage development of one set of veins within an orthogonal system of pre-cleavage veins. The examples shown in Fig. 3(a)–(c) illustrate how easy it is to misinterpret the relative age of the veins. Without an understanding of vein reactivation and the two-stage history of one set of veins, it might be erroneously concluded that the two sets of veins are mutually cross-cutting. Figure 2(b) & (c) also show how difficult it can be to recognize vein reactivation. In this example, the pre-existing vein is only 5–10 μm wide; this is comparable to the width of individual inclusion bands within crack–seal veins (Ramsay 1980), suggesting the vein formed as a result of a single crack event. Because the pre-existing vein is so thin, it cannot be discerned within the reactivated part of the vein. In this particular example, syn-cleavage vein propagation ceased because extension was transferred to an en échelon vein. If, however, syn-cleavage vein propagation were to extend along the entire length of a pre-existing microvein, which is the more general situation, all of the textural evidence for reactivation would be lost.

Vein reactivation may be more common than is currently appreciated: veins form over a range of diagenetic and metamorphic conditions, and rocks typically undergo complex deformation histories. The examples shown in Fig. 3(a)–(c) reveal only some of the possible characteristics of vein intersections that have been modified by vein reactivation. Other geometries are likely, depending upon the relative orientation and age of the pre-existing veins and their orientation with respect to the superposed strain field.

Acknowledgements—This research was supported by National Science Foundation grant EAR-9316334. We thank Joe Bouchard for help in preparing the thin sections and Art Goldstein, Richard Norris and an anonymous referee for reviews that significantly improved the manuscript. Orientation data were plotted using Stereonet v.4.9.6 by Richard W. Allmendinger.

REFERENCES

- Ague, J. J. 1994. Mass transfer during Barrovian metamorphism of pelites, south-central Connecticut. II: Channelized fluid flow and the growth of staurolite and kyanite. *Am. J. Sci.* **294**, 1061–1134.
- Chan, Y. C. & Crespi, J. M. 1995. Noncoaxial strain accumulation and vein reactivation during slaty cleavage development in the northern Taconic Allochthon. *Geol. Soc. Am. Abs. w. Prog.* **27**, 35.
- Chapple, W. M. 1973. Taconic orogeny: abortive subduction of the North American continental plate?. *Geol. Soc. Am. Abs. w. Prog.* **5**, 573.
- Davison, I. 1995. Fault slip evolution determined from crack–seal veins in pull-aparts and their implications for general slip models. *J. Struct. Geol.* **17**, 1025–1034.
- Dunne, W. M. & Hancock, P. L. 1994. Palaeostress analysis of small-scale brittle structures. In: *Continental Deformation* (edited by Hancock, P. L.). Pergamon, Oxford, 101–120.

- Groshong, R. H. Jr. 1988. Low-temperature deformation mechanisms and their interpretation. *Bull. geol. Soc. Am.* **100**, 1329–1360.
- Orange, D. L., Geddes, D. S. & Moore, J. C. 1993. Structural and fluid evolution of a young accretionary complex: the Hoh rock assemblage of the western Olympic Peninsula, Washington. *Bull. geol. Soc. Am.* **105**, 1053–1075.
- Ramsay, J. G. 1980. The crack–seal mechanism of rock deformation. *Nature* **284**, 135–139.
- Rowley, D. B., Kidd, W. S. F. & Delano, L. L. 1979. Detailed stratigraphic and structural features of the Giddings Brook Slice of the Taconic Allochthon in the Granville area. In: *New York State Geological Association and New England Intercollegiate Geological Conference Guidebook for Field Trips* (edited by Friedman, G. M.). Rensselaer Polytechnic Institute, Troy, New York, 186–242.
- Stanley, R. S. & Ratcliffe, N. M. 1985. Tectonic synthesis of the Taconian orogeny in western New England. *Bull. geol. Soc. Am.* **96**, 1227–1250.
- Wallis, S. R. 1992. Vorticity analysis in a metachert from the Sanbagawa Belt, SW Japan. *J. Struct. Geol.* **14**, 271–280.
- Zen, E. -An 1961. Stratigraphy and structure at the north end of the Taconic Range in west–central Vermont. *Bull. geol. Soc. Am.* **72**, 293–338.